



# A multi-scale physical model of granular materials

Annie Luciani, Arash Habibi, Emmanuel Manzotti

## ► To cite this version:

Annie Luciani, Arash Habibi, Emmanuel Manzotti. A multi-scale physical model of granular materials. Graphics interface' 95, 1995, Québec, Canada. pp.136-146. hal-00910588

**HAL Id: hal-00910588**

**<https://hal.science/hal-00910588>**

Submitted on 22 May 2014

**HAL** is a multi-disciplinary open access archive for the deposit and dissemination of scientific research documents, whether they are published or not. The documents may come from teaching and research institutions in France or abroad, or from public or private research centers.

L'archive ouverte pluridisciplinaire **HAL**, est destinée au dépôt et à la diffusion de documents scientifiques de niveau recherche, publiés ou non, émanant des établissements d'enseignement et de recherche français ou étrangers, des laboratoires publics ou privés.

## A Multi-Scale Physical Model Of Granular Materials

A. Luciani, A. Habibi, E. Manzotti

ACROE - LIFIA

INPG - 46 avenue Félix Viallet  
38 031 Grenoble cedex FRANCE

e-mail : <luciani@imag.fr>

Tel : (33) 76 57 46 69

Fax : (33) 76 57 46 02

### Résumé

Les matériaux granulaires ont fait l'objet de nombreuses études. Pourtant certaines de leurs propriétés sont encore très mal comprises. Certaines propriétés tiennent de celles des fluides, d'autres tiennent de celles des solides et encore d'autres ne tiennent ni des uns ni des autres. On a parlé d'un "quatrième état de la matière". C'est sans doute précisément la raison pour laquelle ces matériaux sont aussi fascinants et beaux pour l'homme. Aussi l'objectif de ce travail est, d'une part la compréhension des comportements de ces matériaux en fonction des propriétés de chaque grain, et d'autre part, l'obtention d'animations réalistes et belles par la simulation physique de ces grains. La modélisation multi-échelles des matériaux granulaires consiste à réaliser des modèles physiques distincts et à les coupler pour obtenir la simulation finale. Chacun de ces modèles tient compte d'un type particulier de phénomène (linéaire, non-linéaire, chaotique etc.) et surtout à une échelle temporelle, spatiale ou matérielle différentes. Cette approche nous permet d'obtenir en un temps raisonnable une simulation physique correcte, même pour des phénomènes dynamiques à petite échelle.

### Abstract

Granular materials display a certain number of properties that have long been observed but only partially understood. Some resemble the properties of solids, some resemble properties of fluids and others are unique. The concept of "fourth state of matter" has been mentioned. This is perhaps precisely the reason why these materials are so fascinating and beautiful. Thus the aim of this work is both a better physical understanding of the causes of these phenomena in terms of the properties of individual grains, and the achievement of realistic and beautiful animation

sequences by the physical simulation of these grains. Multi-scale physical modeling of granular materials consists of elaborating several separate component physical models and coupling them in order to obtain the final dynamic animation sequence. Each component model is associated with a specific type of phenomenon (linear, non-linear, chaotic etc.) and above all, with a specific scale or discretization level in time, in space or in matter. This type of modeling enables us to obtain, in a quite reasonable time, a physically correct simulation even for small-scale dynamic phenomena.

Keywords : Physical modeling, Point physics, Phyxels, Refinement.

### 1. Introduction

Sugar, flour and sand are examples of familiar granular materials. They are also frequently handled in industries such as pharmaceuticals and the construction of highways and dams. In spite of all this, and in spite of the beautiful shapes and movements produced by these objects, their dynamic behavior, particularly phenomena such as piling, avalanches, internal collapses, and arching are not very well understood. Therefore our aim is not to model directly any given macroscopic phenomenon, but to carry out a series of experiments on large numbers of physically simulated grains and to determine the causes of the observed phenomena in terms of the physical properties of the individual grains.

Even when the causes of the macroscopic phenomena have been determined, the simulation itself can still be computationally expensive. The various involved phenomena are of very different natures (linear, non-linear, chaotic or not etc.) and different scales. This means that each requires a different





discretization of time, space or matter. This is why, it is often considered that a physically correct simulation of all these phenomena at the same time requires simultaneously a very complex model, and very fine spatial and time discretizations. Thus, current simulations often present a very limited set of these phenomena. [1] [2] [3] [4] [5]

Multi-scale modeling consists of taking advantage of these very disparities. Modeling granular materials involves intermediate-scale non-linear phenomena on the one hand and small-scale linear phenomena on the other. Instead of making one very expensive, finely discretized non-linear physical model that will cope with the requirements of both types of phenomena, multi-scale modeling consists of making several separate models : one intermediate-scale non-linear physical model, and one finely discretized linear physical model. The final animation sequence is obtained by coupling these two models.

In section 2 we will present several experimentally observed characteristics and properties of real granular materials. These properties were used for the evaluation of our models. Section 3 is an overview of the current models of such materials in the physics and computer graphics literature. We modeled and simulated our grains using the *Cordis-Anima* system [6] [7]. Section 4 is a short introduction to *Cordis-Anima*, and to the physical models used in this paper. In section 5 we will present the minimal models and conclusions resulting from our experimentation. Section 6 presents the finely discretized linear model and the link with the previous intermediate-scale non-linear model.

## 2. Granular Materials : Special Properties

Sand and other granular materials are composed of solid particles. However, they cannot be easily classified as either solids or liquids. Their overall shape is the shape of their container and they can also flow out of the container as do liquids. Still, they have several particular properties that can definitely not be explained by classical fluid mechanics.

a. As it is explained in [1], the pressure at the bottom of a sufficiently tall container, filled with sand up to a height  $h$  is independent of  $h$ . For a liquid, pressure is proportional to  $h$ . This is because the friction of the particles along the wall of the container is sufficient to withstand the weight of the extra mass placed on its top. For this reason, in an hourglass filled with fine sand, there is an approximate linear relation between filling height and draining time.

b. When sand is poured on a flat surface, it forms a pile i.e. a characteristic shape of the material and not of any container. (Of course this does not occur for fluids)

c. As distinct from liquids, granular heaps are stationary as long as the top surface is at a slope less than the rest angle  $\theta_r$ . No avalanches spontaneously occur until the slope is increased above the "maximum angle of stability"  $\theta_m$ . When the slope is increased slightly above  $\theta_m$  grains begin to flow and an avalanche of particles occurs. Between  $\theta_r$  and  $\theta_m$  is a region of complex, bistable behavior in which the material can be either stationary or flowing.

d. In a gas or in a liquid at finite temperatures, pressure is a continuous isotropic function of space because of the thermal motion. Conversely there is almost no thermal motion in granular materials. Therefore granular materials are inherently inhomogeneous and the force network providing the stability of the system is nonuniform. Lines conveying high constraints surround regions where pressure is almost zero. [1] [8]

e. Granular materials show a phenomenon known as *arching*. In a random configuration of grains, there will be places where arches appear naturally, leaving empty regions below [1] [4].

f. In some conditions, at the breaking of the force lines mentioned in d, entire *subpiles* collapse within the pile.

These are the major non-linear phenomena that can be considered as specifically granular. In what follows, they will be used for the evaluation of our models.

## 3. Granular Materials : Current Models

The various approaches can be classified as granular or non-granular.

### 3.1. Non-Granular Models

The non-granular approaches use emergent properties; not inherent in one particle but inherent in a large group of particles. This may lead to models in which the granular object is considered as a continuous body, or composed of discrete particles, but which deal with global emergent magnitudes such as slope or statistical magnitudes such as pressure or temperature.

Xin Li and J.M. Moshell [2] have discretized a sand pile in homogeneous continuous vertical columns. The sand on the top of each column can slide to a neighboring columns and produce avalanches. This model does not account for any internal phenomena such as collapses.





Statistical mechanics have also been used to model granular phenomena [8] [10] but this requires that the motion of the grains can be considered as thermal motion. Thus these methods do not tolerate stability and therefore cannot account for phenomena such as piling or arching.

Bak, Tang and Wiesenfeld [3] have elaborated cellular automata sandpile models based on an analogy between avalanches in sandpiles and second order phase transitions. Whatever their value, these models deal with different arrangements of grains but not with dynamics.

### 3.2. Granular Approaches

In this approach, granular materials are explicitly considered as a set of discrete particles locally interacting with the neighboring particles regardless of any consideration on slope or pressure. Geometrical simulations have led to experimental results as for the compacity of granular materials and arching possibilities [1] [4]. But as the authors emphasize, these simulations do not account for important dynamic phenomena such as avalanches.

In the field of computer graphics, discrete models have been used mostly for the simulation of highly deformable objects such as fluids. Terzopoulos et al. [10] have adopted a molecular dynamic approach in which material points are linked by "thermo-elastic units" conveying heat and mechanical forces. The elasticity of these units decrease as the temperature rises. In the molten state, the interaction between the points is characterized by long-range attraction and short-range repulsion (Lennard-Jones interaction). This enables to simulate the melting of a solid object in high temperatures. Miller and A. Pearce have achieved a granular dynamic model [5]. Such as in [10] and in [11], the interaction model between the grains is of the Lennard-Jones type. The grains are poured on fixed circular "constraints" with impulse-based interactions with the grains.

Greenspan [12] considers modeling as an intermediate step between the discrete data obtained from scientific experiment and the discrete data obtained by numerical simulations. In accordance with Greenspan, we believe that discrete models are much more constant than continuous models, not only for highly deformable objects, but in the general context of numerical simulations. All our previous works (including the modeling of either rigid or deformable objects) have been carried out with discrete models based on point physics. The work presented in this paper corresponds definitely to a granular approach. A

granular material is explicitly modeled as a set of discrete masses in physical interaction with other grains and with the ground surface. There are no impulse-based interactions or punctual contacts. This proved to be very important, especially for the interactions with the ground. But the novelty of our approach is firstly in the approach that consists in the research of all the observed phenomena stated in section 2, secondly in the research of the most necessary elements of the model as well as minimal discretizations, and thirdly in multi-scale modeling, which enabled us to carry out one very expensive simulation in two very cheap steps.

### 4. Cordis-Anima Models

The simulations were achieved thanks to the *Cordis-Anima* modeler-simulator [6] [7]. This means that any physical scene or object is modeled only with two basic algorithmic cells : <MAT> and <LIA>. Thus a physical model is a network of <MAT> elements linked by <LIA> elements.

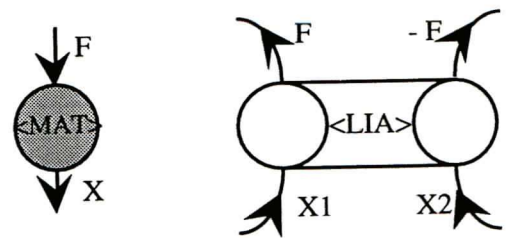


figure 4.1 The <MAT> and the <LIA> element, the two atoms of *Cordis-Anima*

These are dual elements, <MAT> reads a force vector and yields a position. <LIA> reads a pair of positions or velocities and yields to opposite force vectors. Both algorithms can be defined arbitrarily. However, the <MAT> algorithm used in this paper is the mass algorithm, (Newton's second law) and those used for the <LIA> algorithm are the linear visco-elastic interaction  $F_L$ , and the non-linear visco-elastic collision interaction  $F_{NL}$ .

$$\langle \text{MAT} \rangle : \vec{X} = \iint \frac{\Sigma \vec{F}}{m} dt^2$$

$$\langle \text{LIA} \rangle : \vec{F}_L = \left( -k \cdot (d_{12} - d_0) - z \cdot \frac{d}{dt} (d_{12}) \right) \cdot \vec{u}_{12}$$

$$\langle \text{LIA} \rangle : \begin{cases} \vec{F}_{NL} = \vec{F}_L & \text{if } d_{12} \leq d_0 \\ \vec{F}_{NL} = 0 & \text{if } d_{12} > d_0 \end{cases}$$



where  $\vec{u}_{12} = \frac{\vec{X}_2 - \vec{X}_1}{|\vec{X}_2 - \vec{X}_1|}$  and  $d_{12} = |\vec{X}_2 - \vec{X}_1|$ ,

$k$ ,  $z$ , and  $d_0$  are respectively the stiffness, the damping factor and the rest length of  $F_L$  and  $F_{NL}$ . The characteristics of these interaction functions are on figure 4.2.

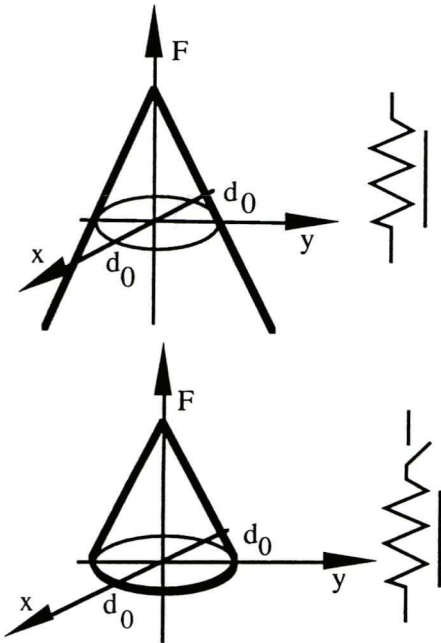


**figure 4.2** Characteristics and symbols of the linear spring-damper and the non-linear visco-elastic interaction.

## 4.2. Grain Models

### 4.2.1. Smooth One Point Grains

The simplest grain model is a *Cordis - Anima* mass element in non-linear visco-elastic collision interaction with all the other grains and with the ground. This interaction generates a visco-elastic non-penetration volume, that determines the shape of the mass. When the mass is free, this volume is a sphere. When it enters in interaction with another mass, the distance between both points is determined by the non-linear physical interaction. Unlike rigid objects, this distance can get smaller than  $d_0$ . During the collision time, the relative motion of both masses may be oscillating or damped, (possibly with micro-collisions if the sampling period is small enough) depending on the parameters of the interaction function, on the value of both masses and more generally on the physical context of the scene if other masses are involved. Impulse-based interactions can definitely not account

for such complex non-linear behavior since they assume zero collision times and punctual contacts. This holds also for more grains (figure 4.3) The distance between each pair of masses varies in its own characteristic way depending on each of the corresponding interactions. This is why the objects undergo non-isotropic deformation and, above all, the deformability of the global object is not the same in all directions. This proved to be very important as this is also the case with granular materials.

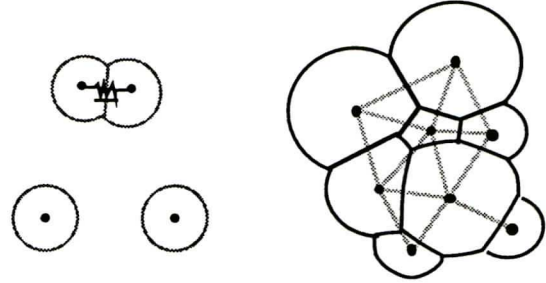


**figure 4.3** One point grains and their deformations

### 4.2.2. Smooth Multi-Point Grains

By attaching several matter points together by linear visco-elastic interactions, we modeled deformable grains with more complex non-penetration volumes, and with possibly non-radial reaction forces. These grains are characterized by a finite pattern-factor. Finite pattern-factors can cause interlocking between grains and facilitate arching [1] (figure 4.4)

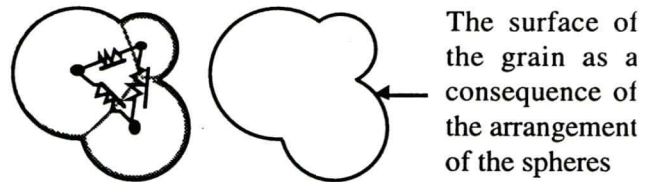


**figure 4.4** the structure of multi-point grains

### 4.2.3. Rugged One-Point Grains

A. Luciani and S. Jimenez [13] have modeled one point grains in non-linear visco-elastic collision interaction, as in 4.2.1, but also with dry friction (as opposed to viscous friction) between the grains. This model was also used in our experimentation.

## 4.3. Ground Surface Models

We have modeled smooth flat grounds and rugged flat grounds. Smooth surfaces generate normal reaction forces. But once again, these contacts are neither impulsed-based nor punctual. In order to model





rough surfaces, we fixed on a smooth surface, small *Cordis-Anima* matter points in non-linear visco-elastic collision interaction with the grains. These points act as small irregularities that cause friction. This type of surface is characterized by a finite pattern-factor. The emergent angle of internal friction can be controlled by the radius of these irregularities as well as their spatial period, (figure 4.5).

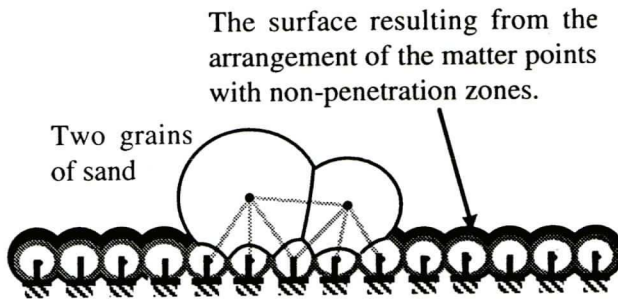


figure 4.5 the rugged surface model composed of matter points acting as irregularities

## 5. Searching For The "Minimal Model"

### 5.1. The Search of Causes

With all these different models, we seek to achieve a simulation in which the phenomena described in section 2 can be observed. Implementing the most complex model of all would perhaps produce all the expected phenomena. However, this would be no satisfactory approach. From a mere computational point of view, this model would clearly not be the cheapest of all. Moreover, this approach does not enable to distinguish the factors that *cause* a given phenomenon and the factors that simply *influence* it. This is why, for each phenomenon (piling, arching, avalanches ...), we look for the "minimal model", representing the necessary conditions in which this phenomenon can be observed. For example the minimal model for piling is a model such that any

simpler model would not produce piling. Thus the *causes* of piling are *contained* in this minimal model and studying the causes of piling boils down to the study of its minimal and cheapest model.

### 5.2. Experimentations and Results

We carried out a series of experiments pouring different types of simulated grains on different types of simulated ground surfaces and checking whether a pile was formed or not. The results of these experimentations were quite unexpected : If the ground on which the grains are poured is smooth, no pile is formed, whatever the grain model. But the converse is also true : if the ground is sufficiently rugged, the grains form necessarily a pile. This is true even for round, smooth, non-viscous, non-adhesive grains i.e. the simplest model of grain (figure 5.1).

### 5.3. The minimal model

The minimal model for piling turns out to be a rather simple model :

1. round, smooth, non-viscous grains
2. in non-linear elastic collision interaction
3. poured on a sufficiently rugged ground
4. in a lowly viscous environment
5. with a rather low number of masses (between 300 and 1000)

But this rather simple model accounts also for nearly all the phenomena described in section 2 :

a. The velocity of the grains flowing out of the hourglass is constant, whether the hourglass is full or half full. This means that the pressure at the bottom of the hourglass is also constant

b. A pile is formed.

c. The slope of the pile increases up to a critical value depending on the stiffness of the grains. If more grains are poured on the pile, avalanches occur and the slope of the pile remains beneath this critical value.

d. At a given instant, high pressure zones are

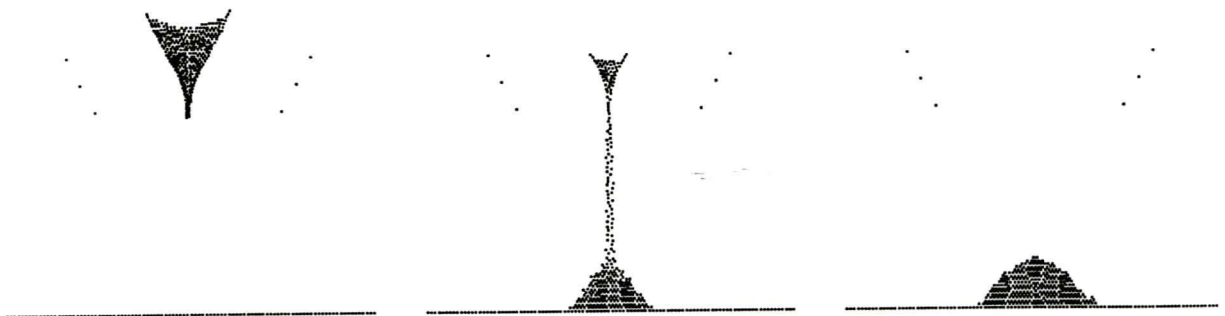


figure 5.1 Three stages of a successful simulation for piling : at  $t = 0$ ,  $t = 3s$  and  $t = 6.4 s$



discrete rows of grains.

e. These rows divide the global pile in internal subpiles. When one of these rows breaks, the surrounding subpiles collapse, causing other collapses above.

f. Arching has been observed

Thus, piling, avalanches and collapses are not caused by the shape of the grains, nor by dry friction between grains, or adhesion. The relevant parameter seems to be the smoothness of the ground. This is a minimal model for the phenomena stated in section 2.

However, more complex behavior can be obtained by more elaborate models. For example using grains of different sizes favours arching and segregation. Using interactions of the Lennard-Jones type increases adhesion and simulates moist sand.

Another important conclusion of the above work concerns discretization. In a real sand pile, there may be millions of grains, whereas in our simulated piles, we observed piling, discrete pressure lines, avalanches and collapses with only 300 to 1000 grains. This means that for these particular chaotic non-linear phenomena, no finer discretization is required. But this also means that our grains are mere discretization units and that each represents in fact a large number of real grains. The grains described above, are half way between the macroscopic scale of the pile and the small scale of fine sand. This is the reason why, in what follows, they will be called *intermediate-scale grains* as opposed to fine grains.

## 6. 2D Multi-scale modeling

The models described in the previous sections are all 2D instances of 3D models. The refinement technique that we are about to present operates only on 2D simulations. Its generalization to 3D scenes will be discussed further.

### 6.1. dynamic and spatial refinement

For other phenomena, such as flow, or merely for visualization, a far finer discretization is needed. A closely packed set of intermediate-scale grains should yield a practically uniform stretch of sand and a moving intermediate-scale grain represents an elementary area of flowing sand. It should yield a smooth deformable trickle of small grains of sand (figure 6.1). Each intermediate-scale grain is replaced by a set of fine grains. The number of these fine grains and the shape of the set depend on the movement of the intermediate-scale grain. Therefore this requires physical modeling. Since all the typical non-linear properties characterizing sand piles have

already been modeled by the intermediate scale model, our hypothesis is that these small-scale phenomena can be adequately approximated by a linear dynamic model. In these conditions, it would be a redundancy to refine the discretization of a non-linear  $O(n^2)$  model simply to cope with the requirements of linear phenomena.

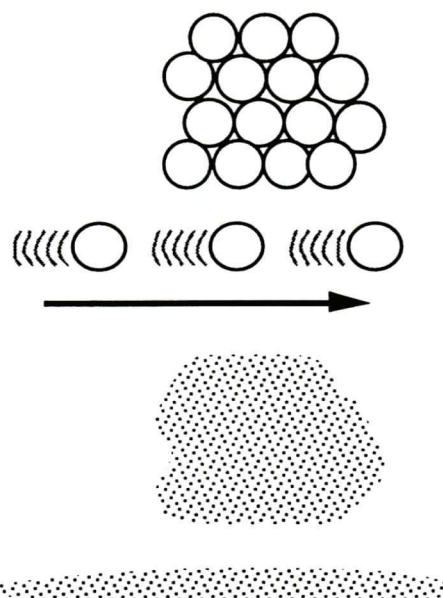


**figure 6.1** The required correspondance between the intermediate-scale non-linear simulation (above) and the final small-scale simulation (below)

The alternative is *multi-scale modeling* : the point is to simulate the non-linear phenomena at their own scale, but to couple this non-linear model with a finely discretized linear dynamic model that will add the linear phenomena to the final sequence. This model is discretized in space, whereas the non-linear model is discretized in particles (figure 6.2)

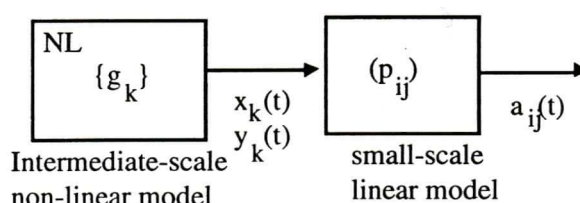


**figure 6.2** The global structure of the model

The scene where the animation takes place is a limited portion of the plane. This portion is discretized by a grid  $P_{ij}$ . The discretization step of  $P_{ij}$  must be smaller than or equal the characteristic spatial frequency of the flow phenomena. At any rate, it must





be much smaller than the discretization of the non-linear phenomena, i.e. distance  $d_{kl}$  between each pair  $(g_k, g_l)$  of intermediate-scale grains. The nodes of this grid are called *phyxels* ( $p_{ij}$ ) as in "physical element".

Each phyxel is characterized by a dynamic variable  $a_{ij}(t)$ . These variables are calculated by the linear system, in terms of the 2D coordinates  $\{x_k(t), y_k(t)\}$  of all the intermediate-scale grains  $g_k$  at instant  $t$ , which are the outputs of the non-linear system. The equations of the linear system are the equations of a homogenous 4 -connex grid of one-dimensional masses placed at  $p_{ij}$ , moving in the  $a_{ij}$  direction. (figure 6.3).

Each mass is linked to a fixed point on the ground by a one-dimensional visco-elastic link, of stiffness  $k_s$  and damping factor  $z_s$  and to each of its four neighbors by the same type of link, of stiffness  $k_i$  and damping factor  $z_i$ .

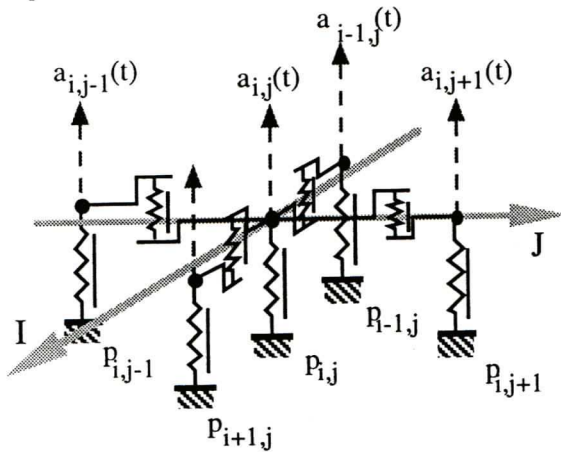


**figure 6.3.** phyxel  $p_{ij}$  linked to its neighbors and to the ground

The equations of the system are as follows.

$$\ddot{a}_{ij} = L_{ij} + \sum_{(l,m) \in G} L_{ij}^{lm} + E_{ij}(x_k, y_k) \quad (1)$$

where  $G = \{(i-1, j), (i+1, j), (i, j-1), (i, j+1)\}$

$$L_{ij} = -k_s a_{ij} - z_s \dot{a}_{ij}$$

$$L_{ij}^{lm} = -k_i (a_{ij} - a_{lm}) - z_i (\dot{a}_{ij} - \dot{a}_{lm})$$

$$E_{ij}(x_k, y_k) = \sum_k e(x_i - x_k, y_i - y_k) \cdot \rho_{ij}^r(x_k, y_k)$$

$$\rho_{ij}^r(x, y, r) = 1 \quad \text{if } (x_i - x_k)^2 + (y_i - y_k)^2 \leq r^2$$

$$\rho_{ij}^r(x, y, r) = 0 \quad \text{if } (x_i - x_k)^2 + (y_i - y_k)^2 > r^2$$

$E_{ij}(x_k, y_k)$  represents the input of the linear system depending on the outputs  $\{x_k(t), y_k(t)\}$  of the non linear system and  $e(x, y)$  is an arbitrarily defined time-independent profile.

Thus equation (1) leads to :

$$\ddot{a}_{ij} = -(k_s + k_i) a_{ij} - (z_s + z_i) \dot{a}_{ij} + \sum_{(l,m) \in G} (-k_i a_{lm} - z_i \dot{a}_{lm}) + E_{ij}(x_k, y_k) \quad (2)$$

This linear model is the  $O(n)$  model thanks to which the intermediate-scale model was refined. It was also elaborated in accordance with the Cordis-Anima formalism.

The solution of equation (2) is a deformation field  $a_{ij}(t)$  depending on the positions  $\{x_k(t), y_k(t)\}$  of the intermediate-scale grains  $\{g_k\}$ . This deformation field will be used for the elaboration of the final image. It has one deformation degree of freedom (dof) in the  $a_{ij}$  direction, and two propagation dofs in the  $i$  and  $j$  directions.

Initially, the scope of the influence of each intermediate-scale grain  $\{g_k\}$  on the deformation field is limited to phyxels located in the immediate vicinity of the involved grain, due to the effect of the  $p_{ij}(x, y)$  function. Subsequently this influence propagates. We define the *zone of influence*  $A_{k,C}(t)$  of the grain  $g_k$  associated with the threshold value  $C$  the set defined as follows (figure 6) :

$$A_{k,C}(t) = \{p_{ij} / a_{ij}(t) < C\}$$

As the system is linear, for several intermediate grains, the total zone of influence is the union of all individual zones of influence. For a given discretization step, the number of phyxels in each  $A_{k,C}(t)$  depends on the parameters of the linear system ( $k_s, k_i, z_s, z_i$ ) and on the  $d_{kl}$  between each pair  $(g_k, g_l)$  of intermediate-scale grains.

The parameters of the linear system have been tuned in such a manner that this zone of influence remains a connex set of phyxels in the vicinity of the intermediate-scale grain. The shape and size of this zone depend on the direction and the speed of this grain. This makes it possible to stretch this shape in the direction of the motion and to generate the shape of an elementary trickle of fine sand. When the intermediate-scale grains are at rest, the linear system may act as a low-pass filter. Thus the zone of influence of a closely packed set of grains is a uniform





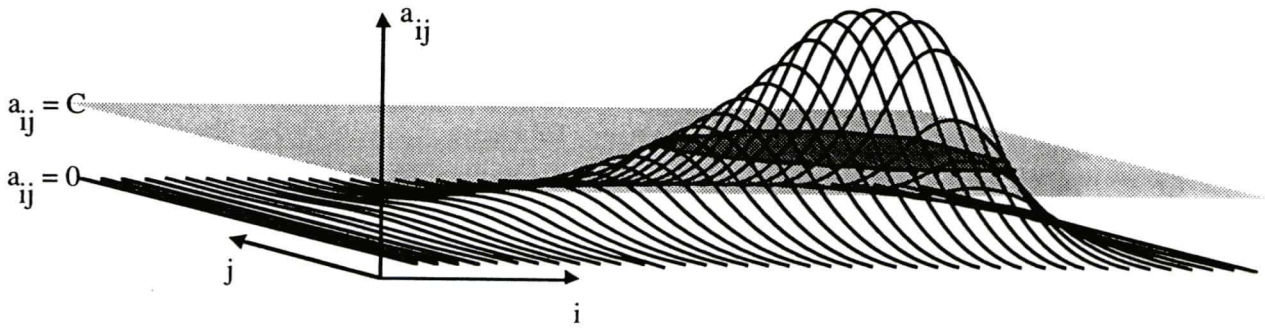


**figure 6.4** - 3D curve representing the deformation field, marked by one intermediate-scale grain  $\{g_k\}$  moving from left to right. Its zone of influence  $A_{k,C}(t)$  is shaded in dark gray.

stretch of sand, composed of a great number of phyxels.

## 6.2. Visualization

In the visualization process, each phyxel is associated with one or several pixels on the visualization screen. For a video format image, there may be up to  $768 \times 576 = 442\,368$  phyxels, that is, one phyxel for each pixel. The color of each pixel is determined by the deformation value  $a_{ij}(t)$  of the associated phyxel  $p_{ij}$ , and also possibly by the deformation value of its four neighbors. This relation is determined by a user-defined arbitrary lighting function named *Chroma*. This determines the color of all the pixels associated with a *phyxel*. For all the figures displayed at the end of this paper we have chosen the following parameters :

$$\begin{aligned} \text{color.red} &= 250 \\ \text{color.green} &= 200 \\ \text{color.blue} &= 170 \\ \text{Chroma}(x,y) \cdot \text{red} &= \\ &\left( -0.45 \cdot \overrightarrow{\text{grad}}_x(z) + 0.55 \cdot \overrightarrow{\text{grad}}_y(z) \right) \cdot \text{color.red} \end{aligned}$$

and so forth for the green and blue components of *Chroma*. If each phyxel is associated with several pixels, the colors of the other pixels are determined by linear interpolation. It can be considered that the phyxels associated with their deformation field represent a physically simulated visualization support placed behind the real visualization screen. This is shown on figure 6.5. On this figure each phyxel is associated with one pixel and vice-versa.

The linear physical model is also named the *Engraved Screen* [14]. And by controlling the parameters of this screen e.g. the tessellation, the

discretization of  $(P_{ij})$ , their mass and the physical parameters of the various spring-dampers, it becomes possible to control the grain, remanence, sensitivity, diffusion, static blur and motion blur etc. of the resulting image.

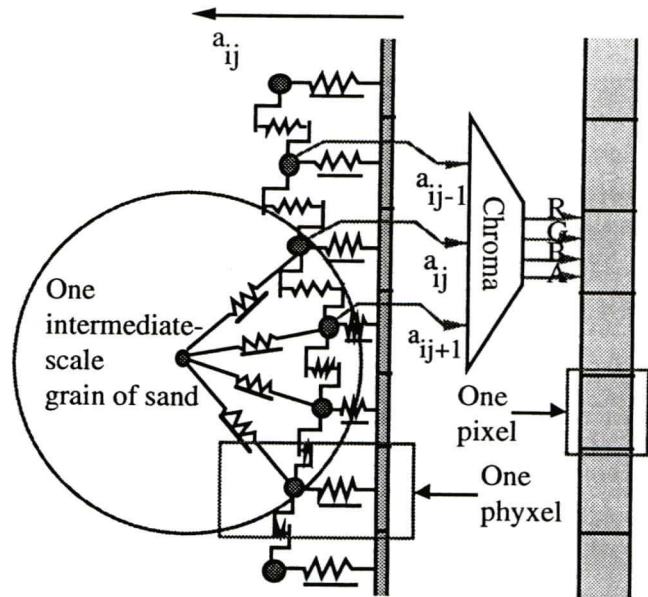


**figure 6.5** Visualization : pixels and phyxels

## 7. Simulations

The results of the simulations described in section 5 are displayed on figures 7.2. and 7.4. These simulations were carried out at 1050 Hz. The models were coupled with the engraved screen and the final results are displayed on figures 7.3 and 7.5

Figure 7.2 represents pebbles blown from left to right by a uniform force field. The grains are deviated by non-linear viscous one-point obstacles and form a dune against a line of fixed visco-elastic obstacles (figure 7.1). These elastic and viscous obstacles were not visualized on the engraved screen visualizations.





For a pebble-like rendering, the *phyxels* are very tightly and viscously attached to the rigid plate. Thus the trace left by each grain does not depend on its motion.

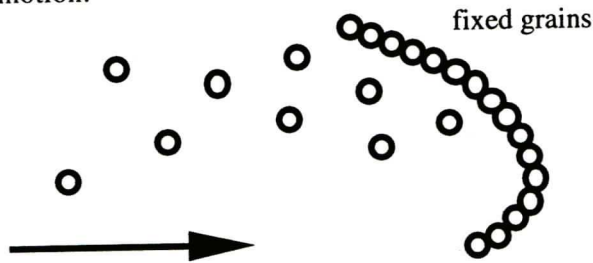


figure 7.1 fixed grains acting as obstacles

On figures 7.4 the grains are blown from left to right in the same manner as above. The refinement model was simulated at 300 Hz. It was composed of  $256 \times 192$  *phyxels*. and its physical parameters :  $(k_s, k_i, z_s, z_i) = (0.03, 0.06, 0.01, 0.01)$ . The stiffnesses are expressed in N/m and the damping factors in N/ms.

For other parameters  $(k_s, k_i, z_s, z_i) = (0.1, 0.01, 1.0, 0.01)$ , the deformation field has non-damped deformation modes, which simulates the behavior of a liquid surface. The refinement of sand with such a model produces a muddy behavior. The muddy consistence cannot appear on a single image. All these simulations will be presented on a video support.

Sequential simulations, with 900 intermediate-scale grains, at the simulation frequency of 300 Hz require 6.625 seconds for each step. (The simulations were carried out on a Silicon Graphics Indigo Extreme). However, the engraved screen algorithm can easily be parallelized and implemented on a massively parallel machine.

The intermediate-scale models are 2D instances of 3D models. Therefore, the achievement of 3D intermediate-scale simulations is straightforward with no additional computational cost. The refinement model can also be extended to 3D. The three-dimensional engraved screen is composed of a 3D network of 1D masses representing a 3D dynamic deformation field. The set of zones of influence generated by objects are projected on the visualization screen. This 3D model is currently being realized.

## 8. Conclusion

To conclude, the novelty of this work is the physical simulation of typically granular phenomena such as piling, avalanches, collapses, arching and the determination of their causes. What is most remarkable, is that all these fine and complex non-linear phenomena were simulated by very simple models : non-linear visco-elastic networks. The

complexity of the simulated phenomena is due to the fine reproduction of the dynamic phenomena and even of oscillations and micro-collisions during the contact time, non-isotropic compression and deformation, etc. This is only possible when the simulation frequency of the macro-scale model is about 1kHz i.e. greater than all the deformation modes associated with these phenomena. Another important result is the achievement of multi-scale physical modeling and the visualization of these phenomena by a physical model with different spatial temporal and matter discretizations. The refinement of the macro-scale model is a linear  $O(n)$  dynamic model.

Finally, we obtain one consistent physically-based model composed of two parts and designed, modeled and simulated with the same *Cordis-Anima* formalism, which enables the cooperation of multi-scale parts of a physically-based model in time and space.

## References

1. M.Ammi, D.Bideau, J.P.Troadec, *Geometrical structure of disordered packings of regular polygons ; comparison with disc packings structures* Journal of Physics D ,vol.20, page 424, 14 April 1987 4.
2. Xin Li, J. Michael Moshell *Modeling Soil : Realtime dynamic Models for Soil Slippage and Manipulation* Proceedings of SIGGRAPH '93
3. P. Bak, C. Tang, K. Wiesenfeld, *Phys. Rev. Lett.* 59, 381 (1987)
4. J.M. Missiaen *Etude par analyse d'images des milieux granulaires : caractérisation des contacts et de l'homogénéité* PhD Thesis. Ecole Nationale Supérieure des Mines de Saint-Etienne (Saint-Etienne 1989)
5. G. Miller A. Pearce *Globular dynamics : a connected particle system for animating viscous fluids.* Computer & Graphics Vol 13, No. 3, pp 305-309 1989
6. C. Cadoz, A. Luciani, JL Florens, *CORDIS-ANIMA : A Modeling and Simulation System for Sound and Image Synthesis - The General Formalism*, Computer Music Journal, 1993,10(1), 19-29, M.I.T. Press
7. A. Luciani, S. Jimenez, C. Cadoz, JL. Florens, O. Raoult, *Computational Physics : A Modeler-Simulator for Animated Physical Objects*, Proceeding of Eurographics Conference, 1991, Vienna, Austria
8. H.M. Jaeger, R. S.R. Nagel *Physics of the granular state* Science vol. 255, page 1523, 20 March 1992





9. S.F. Edwards, A. Mehta, *Dislocations in amorphous materials* Journal de Physique (Paris) vol. 50, page 2489, 15 September 1989. A. Mehta, S.F. Edwards, Phys. A, 157, 1091, 1989.

10. D. Terzopoulos, J. Platt, K. Fleischer *Heating and Melting Deformable Models (From Gloop to Glop)* Proceedings of Graphics Interface '89 London ON, Canada June 1989 page 219-226.

11. A. Luciani, S. Jimenez, O. Raoult, C. Cadoz, JL Florens, *An unified view of multitude behaviour, flexibility, plasticity and fractures: balls, bubbles and agglomerates* - Modeling in Computer Graphics, 1991, 54-74, Springer Verlag Ed..7

12. D. Greenspan *Discrete Models* Addison-Wesley, Reading, M.A, 1973

13. S. Jimenez, A. Luciani, *Animation of Interacting Objects with Collisions and Prolonged Contacts*. Modeling in Computer Graphics 1993 129-141. Springer Verlag Ed.

14. A. Habibi A. Luciani *Physical models for the visualization of animated images "From the physical model to the eye"* Proceedings of the Fourth Eurographics Animation and Simulation Workshop" (Barcelona, Spain September 4-5 1993)

**figure 7.2.** Pebbles flowing from left to right and forming piles against four obstacles

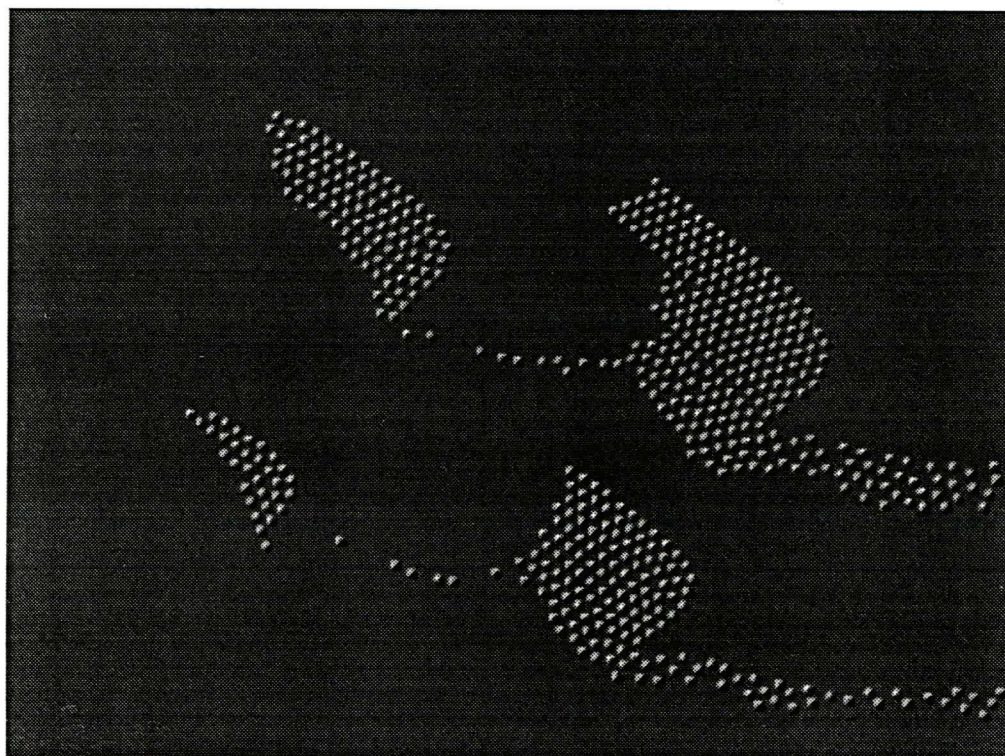
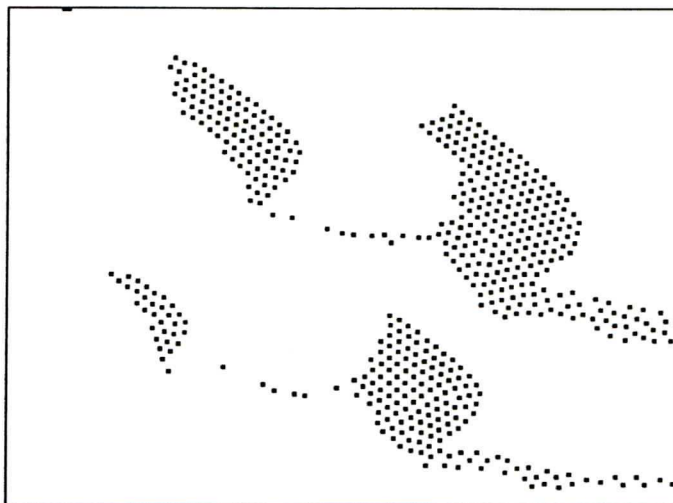


**figure 7.3** The engraved screen refinement of the above model





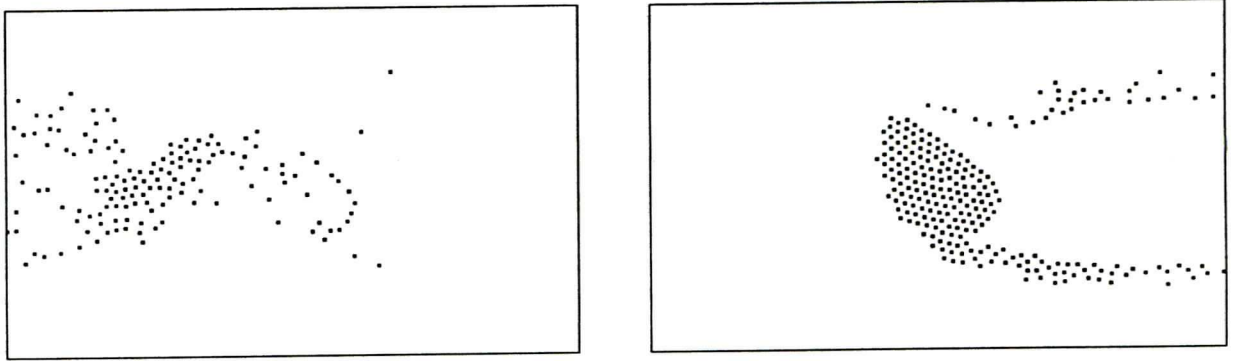


**figure 7.4** Fine sand flowing from left to right and forming a dune against an obstacle (at  $t=1s$  and  $t= 7.8s$ )

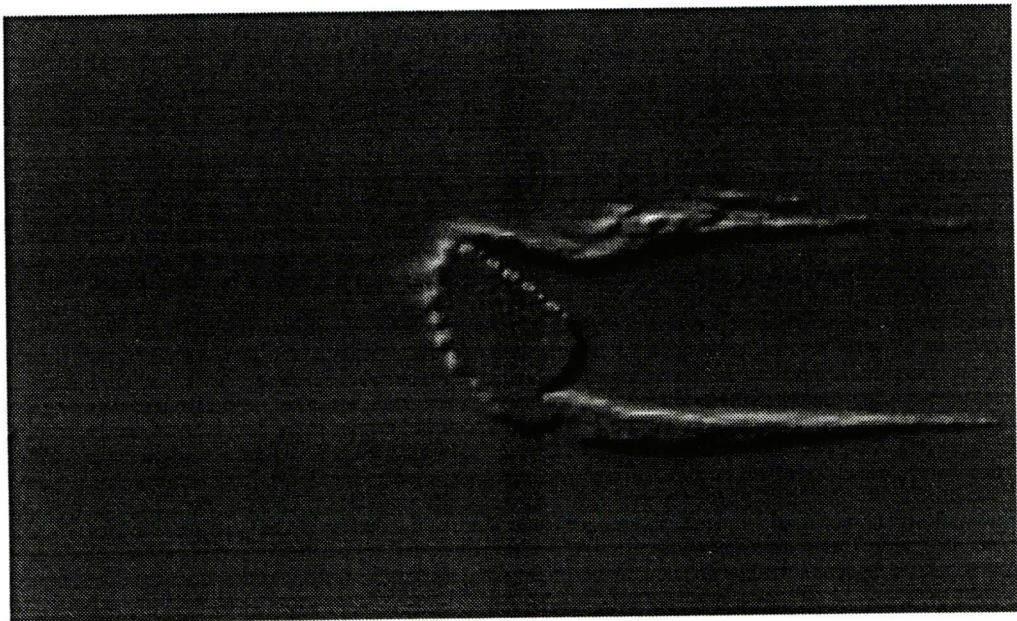
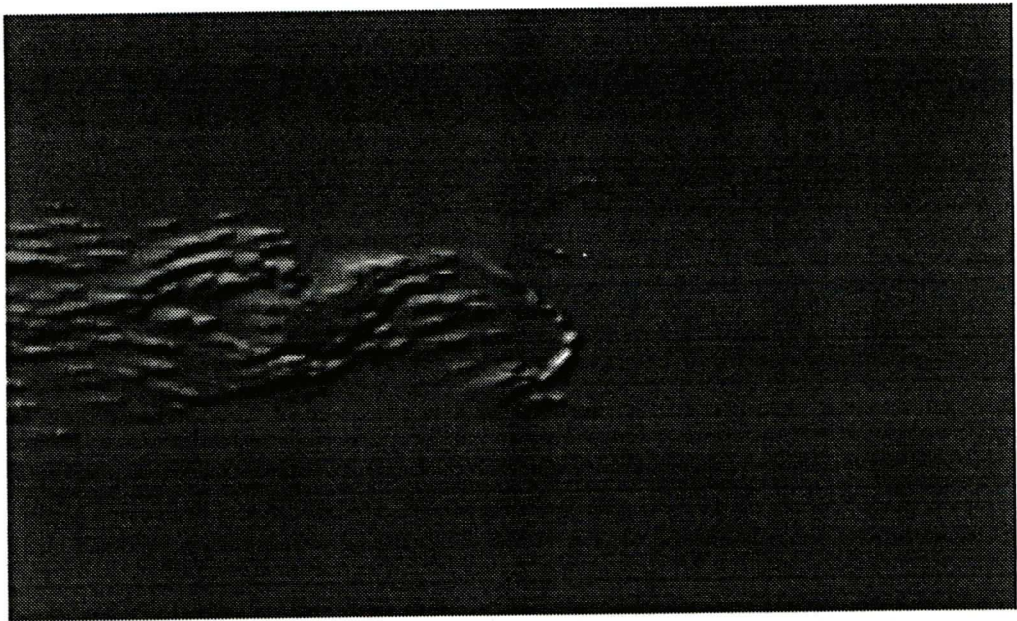


**figure 7.5** The engraved screen refinement of the above model at the same instants

